

Topological flat Wannier-Stark bands

A. R. Kolovsky,^{1,2,3} A. Ramachandran,³ and S. Flach³

¹*Kirensky Institute of Physics, 660036 Krasnoyarsk, Russia*

²*Siberian Federal University, 660041 Krasnoyarsk, Russia*

³*IBS Center for Theoretical Physics of Complex Systems, 34051 Daejeon, South Korea*



(Received 19 July 2017; revised manuscript received 28 November 2017; published 16 January 2018)

We analyze the spectrum and eigenstates of a quantum particle in a bipartite two-dimensional tight-binding dice network. In the absence of a dc bias, it hosts a chiral flatband with compact localized eigenstates. In the presence of a dc bias, the energy spectrum consists of a periodic repetition of one-dimensional energy band multiplets, with one member in the multiplet being strictly flat. The corresponding flatband eigenstates cease to be compact, and are localized exponentially perpendicular to the dc field direction, and superexponentially along the dc field direction. The band multiplets are characterized by a topological quantized winding number (Zak phase), which changes at specific values of the varied dc field strength. These changes are induced by gap closings between the flat and dispersive bands, and reflect the number of these closings.

DOI: [10.1103/PhysRevB.97.045120](https://doi.org/10.1103/PhysRevB.97.045120)

I. INTRODUCTION

Recently, much attention has been paid to flatbands in one-, two-, and three-dimensional lattices with short-range hoppings and nontrivial geometry [1]. Flatbands with finite range hoppings exist due to destructive interference leading to a macroscopic number of degenerate compact localized eigenstates (CLS), which have strictly zero amplitudes outside a finite region of the lattice [2]. Flatband networks have been proposed in one, two, and three dimensions and various flatband generators were identified [3–6]. For bipartite lattices, the existence of flatbands and CLS is ensured through a proper usage of the protecting chiral symmetry [6]. For the dice lattice shown in Fig. 1(a), the CLS consists of an empty C site which is surrounded by six excited A and B sites with alternating amplitudes $\pm 1/\sqrt{6}$. Experimental observations of flatbands and CLS were reported for photonic waveguide networks [7–15], exciton-polariton condensates [16–18], and ultracold atomic condensates [19,20].

In the present paper, we report on a new family of flatbands which exist in dc biased bipartite lattices and which are *not* supported by CLS, despite the short-range hopping. With a dc field added, the Bloch spectrum of a quantum particle transforms into a Wannier-Stark (WS) spectrum and the particle starts to experience well-known Bloch oscillations in the direction of the dc bias (see, e.g., Refs. [21,22]). Our results are applicable for ultracold atoms in optical lattices where the electric field is substituted by a tilt of the lattice in the gravitational field [23] or by accelerating the whole lattice [24]. The same type of perturbations can be arranged in optical waveguide arrays where the electric field is modeled by a curved geometry of the waveguides [25].

II. MODEL

As a particular bipartite lattice, we consider the dice lattice with the dc bias (tilt) along the y direction, see Fig. 1(a). The dice lattice shares similarities with the two-band chiral honeycomb lattice, whose WS spectrum and Bloch oscillations

were studied in Ref. [26]. Unlike the honeycomb lattice, the three-band dice lattice is bipartite *with* a majority sublattice, which ensures existence of a flat Bloch band supported by CLS, see Fig. 1(b) [6]. In what follows, we prove that, when

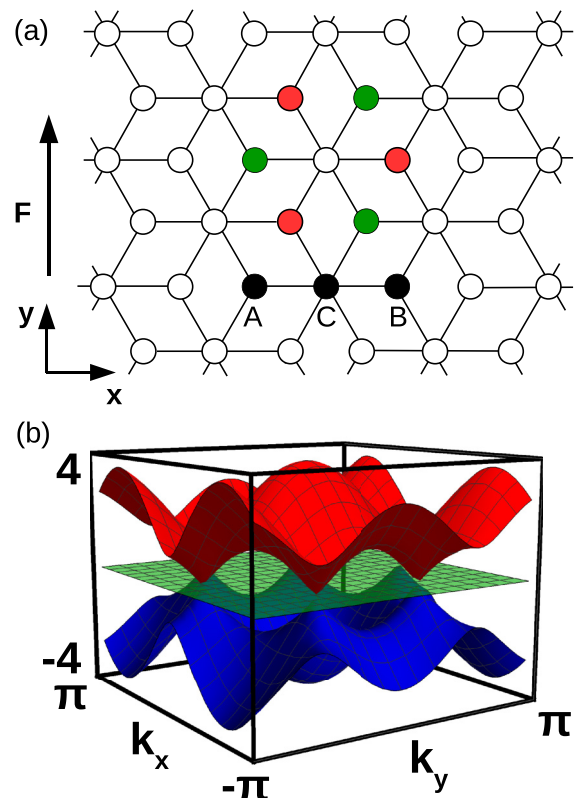


FIG. 1. (a) The dice lattice with the elementary cell consisting of three sites denoted by A , B , and C . The red and green circles represent the amplitudes $+1/\sqrt{6}$ and $-1/\sqrt{6}$, respectively, of a compact localized state. The black sites indicate an uncoupled trimer in the limit of infinitely strong dc bias. (b) Bloch bands of the dice lattice with a flatband at $E = 0$ (for zero dc bias).

a dc field is added, this two-dimensional flat Bloch band generates a ladder of one-dimensional flat WS bands, which are supported by noncompact *exponentially* localized states. Furthermore, these flat WS bands are shown to be topologically nontrivial and are characterized by nonzero integer winding numbers (Zak phase), similar to the Su-Schrieffer-Heeger (SSH) chain [27]. However, at variance to the SSH model with only one topological transition, varying the dc field strength leads to a whole sequence of topological transitions with winding number changes when passing through conical intersection point degeneracies.

It is instructive to start with the limit $|\mathbf{F}| = F \rightarrow \infty$. Then the particle energy is given by a WS ladder of triplets $(-\sqrt{2}t + ndF, ndF, \sqrt{2}t + ndF)$. Here t is the hopping strength and $d = \sqrt{3}/2$ is the Stark lattice period in units of the fundamental lattice period, i.e., the distance between rows of sites with the same Stark energy. The integer n counts the ladder steps. A quantum particle is confined to uncoupled trimers $A - C - B$ shown with black circles in Fig. 1(a). For finite values of F , the particle can tunnel to neighboring rows. Recovering of tunneling together with translational symmetry allows us to search for the particle eigenstates as Bloch waves in the direction orthogonal to \mathbf{F} [26,28]. This statement is correct for any commensurate orientations of the field, for which \mathbf{F} is parallel to a line connecting any two sites of the lattice separated by a finite distance [26]. The energy spectrum then consists of a ladder of one-dimensional band multiplets—the WS bands. The multiplet number equals the number of Bloch bands in the unbiased case. For the considered example, these bands are shown in Fig. 2(a) for $F = 4$. Every third band is flat. Below we explain the presence of flat WS bands in the energy spectrum and obtain localized states associated with these bands.

III. SPECTRAL PROPERTIES

The stationary Schrödinger equation for the biased dice lattice reads

$$E\Psi(\mathbf{R}_j) = (\mathbf{F} \cdot \mathbf{R}_j)\Psi(\mathbf{R}_j) - t \sum_m \Psi(\mathbf{R}_j + \mathbf{r}_m), \quad (1)$$

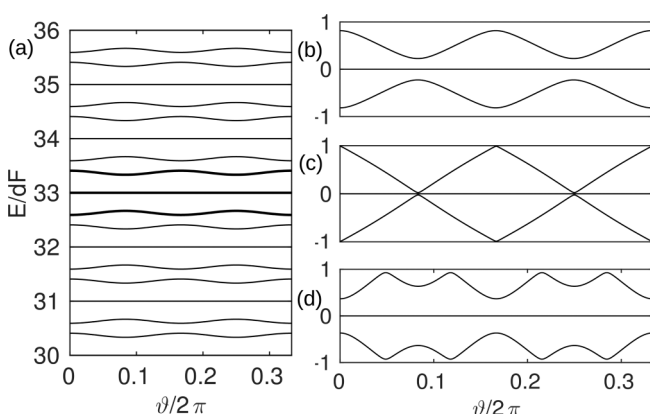


FIG. 2. (a) WS band ladder of the biased dice lattice with \mathbf{F} along the y axis, $F = 4$. Thick lines highlight the irreducible triplet of three WS bands. (b)–(d) Irreducible triplets for (b) $F = 2$, (c) $F = 1/0.62$, and (d) $F = 1$.

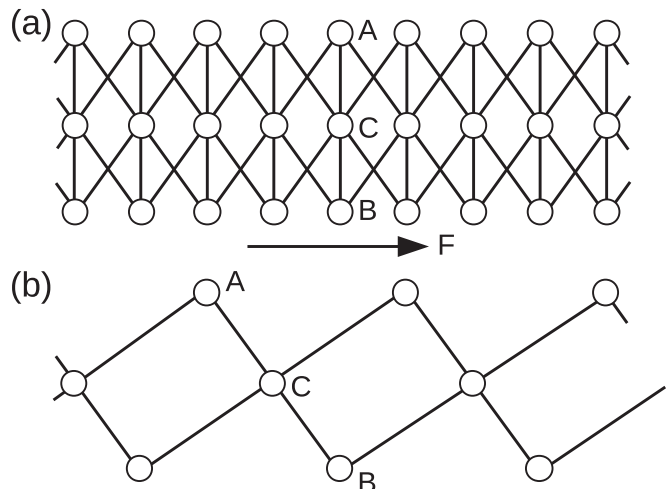


FIG. 3. The dual ladder system for the dice lattice: (a) tilted in the y direction and (b) in the x direction.

where \mathbf{R}_j are the lattice site positions and $|\mathbf{r}_m| = 1$. The sum over \mathbf{r}_m connects three neighboring sites for A or B sites and six neighboring sites for C sites (see Fig. 1). Keeping in mind that \mathbf{F} is parallel to the y axis, we use the substitution $\Psi(\mathbf{R}_j) \sim \exp(i\kappa R_j^y)\psi(R_j^x)$, where κ is the transverse quasimomentum. That reduces the original eigenvalue problem Eq. (1) to a one-dimensional eigenvalue problem with infinitely many bands:

$$\begin{aligned} E\psi_p^A &= dFp\psi_p^A - t\psi_p^C e^{-i2\vartheta} - t(\psi_{p+1}^C + \psi_{p-1}^C)e^{i\vartheta}, \\ E\psi_p^C &= dFp\psi_p^C - t\psi_p^A e^{i2\vartheta} - t\psi_p^B e^{-i2\vartheta} \\ &\quad - t(\psi_{p+1}^A + \psi_{p-1}^A)e^{-i\vartheta} - t(\psi_{p+1}^B + \psi_{p-1}^B)e^{i\vartheta}, \\ E\psi_p^B &= dFp\psi_p^B - t\psi_p^C e^{i2\vartheta} - t(\psi_{p+1}^C + \psi_{p-1}^C)e^{-i\vartheta}, \end{aligned} \quad (2)$$

where $\vartheta = a\kappa$ and $a = 1/2$ is the distance between columns of sites. The system Eqs. (2) is a three-leg ladder in a static field aligned with the ladder legs, see Fig. 3. This is a general result which holds for any rational orientation of the dc field and any ν -band lattice in two dimensions: in the Bloch representation for the wave vector orthogonal to the dc field, each Bloch wave number yields a dual one-dimensional ν -leg ladder in the direction of the dc field. The precise network connectivity of the dual ladder is depending on the field orientation, see Fig. 3.

IV. WINDING NUMBERS

The eigenvalue problem Eqs. (2) for the dual system can be analyzed using the method of generating functions [29,30]. We introduce the Fourier series expansion of three periodic functions in θ :

$$Y^{A,B,C}(\theta) = (2\pi)^{-1/2} \sum_{p=-\infty}^{\infty} \psi_p^{A,B,C} \exp(ip\theta), \quad (3)$$

and arrange them into a column vector function $\mathbf{Y} = [Y^A, Y^C, Y^B]^T$. Then the system of linear algebraic Eqs. (2) is generated from the following differential equation set:

$$idF \frac{d\mathbf{Y}}{d\theta} = G(\theta; \vartheta)\mathbf{Y}, \quad (4)$$

where

$$G(\theta; \vartheta) = - \begin{pmatrix} E & f & 0 \\ f^* & E & f \\ 0 & f^* & E \end{pmatrix} \quad (5)$$

and $f(\theta; \vartheta) = t \exp(-i2\vartheta) + 2t \cos(\theta) \exp(i\vartheta)$. Consider now the unitary map $\mathbf{Y}(2\pi) = U(\vartheta, E)\mathbf{Y}(0)$, where

$$U(\vartheta, E) = \widehat{\exp} \left[-\frac{i}{dF} \int_0^{2\pi} G(\theta; \vartheta) d\theta \right]. \quad (6)$$

Here $\widehat{\exp}$ indicates time ordering if θ is treated as the time. We are searching for an initial vector $\mathbf{Y}(0)$ and energy E , which satisfy periodicity $\mathbf{Y}(2\pi) = \mathbf{Y}(0)$. This can be achieved by first setting $E = 0$, and computing the eigenvalues λ_j and eigenvectors \mathbf{Y}_j of $U(\vartheta, 0)$ with $j = 1, 2, 3$. Together with the gauge invariance of Eq. (4), it follows that periodicity is obtained for initial conditions $\mathbf{Y}(0) = \mathbf{Y}_j$ and energies

$$E_n^{(j)}(\vartheta) = dFn + i \frac{dF}{2\pi} \ln \lambda_j(\vartheta), \quad -\infty < n < \infty. \quad (7)$$

Next we note that for $E = 0$ the matrix G can be presented in the form $G = \Omega \cdot \mathbf{S}$, where \mathbf{S} is the spin-one operator and $\Omega_z = 0$. Then the unitary operator $U(\vartheta, E = 0)$ is a sequence of infinitesimal rotations around a θ -dependent axis Ω . Since the sequence of rotations reduces to a single rotation around some axis $\tilde{\Omega}$, we find $U = \exp(i\tilde{\Omega} \cdot \mathbf{S})$ with $\tilde{\Omega}_z = 0$. The last equation fixes the algebraic structure of the eigenvectors to

$$\mathbf{Y}_{1,2} = \begin{pmatrix} \pm \frac{1}{2} e^{i\chi} \\ \frac{1}{\sqrt{2}} \\ \pm \frac{1}{2} e^{-i\chi} \end{pmatrix}, \quad \mathbf{Y}_3 = \begin{pmatrix} \frac{1}{\sqrt{2}} e^{i\chi} \\ 0 \\ -\frac{1}{\sqrt{2}} e^{-i\chi} \end{pmatrix}, \quad (8)$$

where the phase $\chi = \chi(\vartheta; F)$ is some function of ϑ and F . The first two eigenvectors in Eqs. (8) correspond to complex-conjugated eigenvalues $\lambda_2^*(\vartheta) = \lambda_1(\vartheta)$, which determine the dispersive WS bands according to Eq. (7). The third eigenvector corresponds to $\lambda_3 = 1$, which determines the flat WS bands. We note that the proof of existence of the flat WS bands does not depend on the details of the dependence $\chi = \chi(\vartheta; F)$. Therefore, flat WS bands exist for any rational orientation of the dc field. It is easy to generalize this statement to any dc-biased chiral lattice with three Bloch bands, like the well-known 2D Lieb lattice [6].

The dispersive bands are sensitive to variations of F . At the same time, the bands have a topological invariant Z —the winding number of the relative phases of the eigenvector components:

$$Z = \frac{1}{2\pi i} \int_0^{2\pi/3} e^{-i\chi} \frac{d}{d\vartheta} e^{i\chi} d\vartheta, \quad Z = 0, \pm 1, \dots, \quad (9)$$

which is related to the notion of Zak's phase [31,32]. The winding number ceases to be well defined whenever a degeneracy $\lambda_j(\vartheta)$ takes place. Thus the quantity Eqs. (9) may change its value at particular values of $F = F_{cr}$ where the dispersive bands develop a conical intersection. This is illustrated in Fig. 4. Fig. 4(a) shows the winding number Eqs. (9) as a function of $1/F$, and Fig. 4(b) the gap between the dispersive bands of the irreducible triplet as a function of both inverse field magnitude and transverse quasimomentum. Conical intersections with vanishing gaps appear as black spots. Their

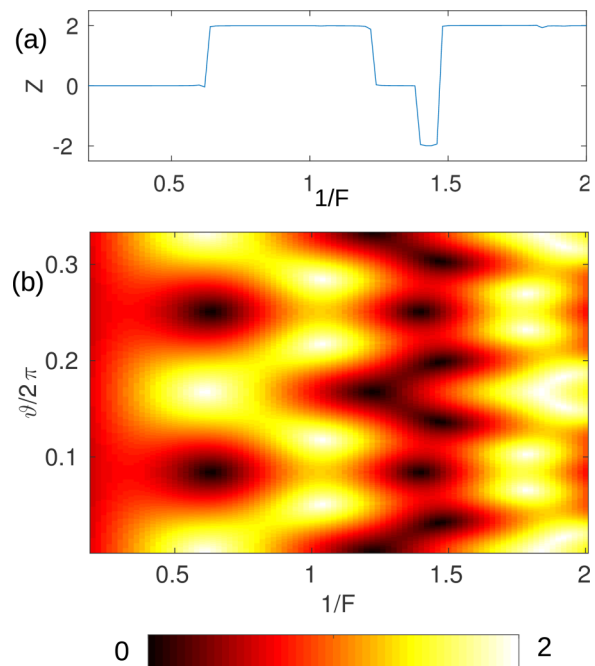


FIG. 4. (a) Winding number of the phase χ as the function of the inverse field magnitude. (b) The gap between the dispersive bands of the irreducible triplet as a function of $1/F$ and ϑ . In this representation, conical intersections and vanishing gaps of the dispersive bands with the parent flatband appear as black spots.

positions and numbers yield the corresponding changes of the winding number Z for the phase $\chi = \chi(\vartheta; F)$ in Eqs. (8). The winding number Z characterizes each triplet of WS bands. Every jump of this number in Fig. 4(a) indicates a topological phase transition. This transition is reflected in a structural change of eigenstates associated with the dispersive bands. Also, the localization length of eigenstates associated with the flatbands diverges as F approaches F_{cr} .

V. LOCALIZED STATES

Let us now discuss the particle eigenstates associated with flat WS bands in more details. Using the vector \mathbf{Y}_3 in Eqs. (8) as an initial condition and evolving it according to Eq. (4), we obtain vector components as the function of two cyclic variables θ and ϑ . Next, taking the Fourier transform of the obtained functions over the variable θ , we obtain site populations of the dual ladder system for a given value of the parameter ϑ . Analogously, taking the two-dimensional Fourier transform over the both cyclic variables we obtain site populations of the original 2D lattice, see inset of Fig. 5. Let us compare the obtained localized state with CLS for $F = 0$. As it was already mentioned, the latter is given by an empty C site surrounded by six A and B sites with alternating amplitudes $\pm 1/\sqrt{6}$. It is seen in Fig. 5 that the center of gravity of the localized state in the tilted dice lattice is also an empty C site. However, the state itself is *not compact*. The results depicted in Fig. 5 with integrated probabilities $P(x) = \int |\Psi(\mathbf{R})|^2 dy$ and $P(y) = \int |\Psi(\mathbf{R})|^2 dx$ on a logarithmic scale, show that the state is exponentially localized in the direction orthogonal to \mathbf{F} and superexponentially in the direction parallel to \mathbf{F} .

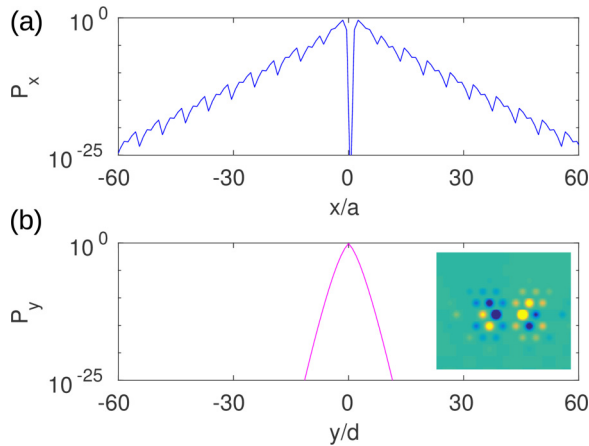


FIG. 5. Integrated probabilities (a) $P(x)$ and (b) $P(y)$ for $F = 4$. Inset: The localized state in the tilted dice lattice for $F = 4$. Occupation amplitudes $\Psi(\mathbf{R}_j)$ of the lattice sites are shown as a color map with dark blue corresponding to -1 and bright yellow to $+1$.

The impossibility to compactify flatband states originates in the presence of the second direction y along the dc field, the “leakage” of the wave function into these directions. That results in a two-dimensional (x, y) wave function corresponding to a one-dimensional (x) periodic lattice. The corresponding localization length is, in general, depending on the dc bias

strength F , and diverges at each topological transition point accompanied by a gap closing and the emergence of conical intersections, signaling the change in topology.

VI. CONCLUSIONS

We can conclude that a 2D tight-binding lattice with ν Bloch bands yields a Wannier-Stark ladder of one-dimensional multiplets of ν bands in the presence of a dc bias with a direction commensurate to the lattice. The bipartite and chiral symmetry of the original lattice is transported into a corresponding one for the WS multiplets. If the chiral symmetry of the original lattice enforces the presence of a flatband which is supported by compact localized states, the WS multiplets will also contain flatbands, which, however, do not support compact states anymore. Tuning of the dc bias leads to changes of a quantized winding number (Zak phase), which characterizes each multiplet. The changes happen precisely when the multiplet is driven through a conical band touching. At these band touchings, the flatband states cease to be localized.

ACKNOWLEDGMENTS

A.K. acknowledges hospitality of IBS Center for Theoretical Physics of Complex Systems, where this work was conducted. This work was supported by the Institute for Basic Science, Project Code IBS-R024-D1.

-
- [1] O. Derzhko, J. Richter, and M. Maksymenko, *Int. J. Mod. Phys. B* **29**, 1530007 (2015).
- [2] S. Flach, D. Leykam, J. D. Bodyfelt, P. Matthies, and A. S. Desyatnikov, *Europhys. Lett.* **105**, 30001 (2014).
- [3] A. Mielke, *J. Phys. A: Math. Gen.* **24**, 3311 (1991).
- [4] H. Tasaki, *Phys. Rev. Lett.* **69**, 1608 (1992).
- [5] W. Maimaiti, A. Andreanov, H. C. Park, O. Gendelman, and S. Flach, *Phys. Rev. B* **95**, 115135 (2017).
- [6] A. Ramachandran, A. Andreanov, and S. Flach, *Phys. Rev. B* **96**, 161104(R) (2017).
- [7] D. Guzmán-Silva, C. Mejía-Cortés, M. A. Bandres, M. C. Rechtsman, S. Weimann, S. Nolte, M. Segev, A. Szameit, and R. A. Vicencio, *New J. Phys.* **16**, 063061 (2014).
- [8] R. A. Vicencio, C. Cantillano, L. Morales-Inostroza, B. Real, C. Mejía-Cortés, S. Weimann, A. Szameit, and M. I. Molina, *Phys. Rev. Lett.* **114**, 245503 (2015).
- [9] S. Mukherjee, A. Spracklen, D. Choudhury, N. Goldman, P. Öhberg, E. Andersson, and R. R. Thomson, *Phys. Rev. Lett.* **114**, 245504 (2015).
- [10] S. Mukherjee and R. R. Thomson, *Opt. Lett.* **40**, 5443 (2015).
- [11] S. Mukherjee and R. R. Thomson, *Opt. Lett.* **42**, 2243 (2017).
- [12] S. Weimann, L. Morales-Inostroza, B. Real, C. Cantillano, A. Szameit, and R. A. Vicencio, *Opt. Lett.* **41**, 2414 (2016).
- [13] S. Xia, Y. Hu, D. Song, Y. Zong, L. Tang, and Z. Chen, *Opt. Lett.* **41**, 1435 (2016).
- [14] B. Real, C. Cantillano, D. López-González, A. Szameit, M. Aono, M. Naruse, S.-J. Kim, K. Wang, and R. A. Vicencio, *Sci. Rep.* **7**, 15085 (2017).
- [15] E. Travkin, F. Diebel, and C. Denz, *Appl. Phys. Lett.* **111**, 011104 (2017).
- [16] N. Masumoto, N. Y. Kim, T. Byrnes, K. Kusudo, A. Löffler, S. Höfling, A. Forchel, and Y. Yamamoto, *New J. Phys.* **14**, 065002 (2012).
- [17] F. Baboux, L. Ge, T. Jacqmin, M. Biondi, E. Galopin, A. Lemaître, L. Le Gratiet, I. Sagnes, S. Schmidt, H. E. Türeci, *et al.*, *Phys. Rev. Lett.* **116**, 066402 (2016).
- [18] C. E. Whittaker, E. Cancellieri, P. M. Walker, D. R. Gulevich, H. Schomerus, D. Vaitiekus, B. Royall, D. M. Whittaker, E. Clarke, I. V. Iorsh *et al.*, [arXiv:1705.03006](https://arxiv.org/abs/1705.03006) (2017).
- [19] S. Taie, H. Ozawa, T. Ichinose, T. Nishio, S. Nakajima, and Y. Takahashi, *Sci. Adv.* **1**, 1 (2015).
- [20] G.-B. Jo, J. Guzman, C. K. Thomas, P. Hosur, A. Vishwanath, and D. M. Stamper-Kurn, *Phys. Rev. Lett.* **108**, 045305 (2012).
- [21] A. R. Kolovsky and H. J. Korsch, *Int. J. Mod. Phys. B* **18**, 1235 (2004).
- [22] O. Morsch and M. Oberthaler, *Rev. Mod. Phys.* **78**, 179 (2006).
- [23] B. P. Anderson and M. A. Kasevich, *Science* **282**, 1686 (1998).
- [24] M. Cristiani, O. Morsch, J. H. Müller, D. Ciampini, and E. Arimondo, *Phys. Rev. A* **65**, 063612 (2002).
- [25] S. Longhi, M. Marangoni, M. Lobino, R. Ramponi, P. Laporta, E. Cianci, and V. Foglietti, *Phys. Rev. Lett.* **96**, 243901 (2006).
- [26] A. R. Kolovsky and E. N. Bulgakov, *Phys. Rev. A* **87**, 033602 (2013).
- [27] J. K. Asbóth, L. Oroszlány, and A. Pályi, *A Short Course on Topological Insulators: Band Structure and Edge States*

- in One and Two Dimensions*, Vol. 919 (Springer, Berlin, 2016).
- [28] T. Nakanishi, T. Ohtsuki, and M. Saitoh, *J. Phys. Soc. Jpn.* **62**, 2773 (1993).
- [29] D. N. Maksimov, E. N. Bulgakov, and A. R. Kolovsky, *Phys. Rev. A* **91**, 053631 (2015).
- [30] D. N. Maksimov, E. N. Bulgakov, and A. R. Kolovsky, *Phys. Rev. A* **91**, 053632 (2015).
- [31] J. Zak, *Phys. Rev. Lett.* **62**, 2747 (1989).
- [32] M. Atala, M. Aidelsburger, J. T. Barreiro, D. Abanin, T. Kitagawa, E. Demler, and I. Bloch, *Nat. Phys.* **9**, 795 (2013).